Published in final edited form as:
Exp Eye Res. 2009 September ; 89(3): 416–425. doi:10.1016/j.exer.2009.04.008.

Absence of SPARC leads to impaired lens circulation

Teri M.S. Greiling[a], **Brad Stone**[b], and **John I. Clark**[c]

Teri M.S. Greiling: teri@u.washington.edu; Brad Stone: bstone@benaroyaresearch.org; John I. Clark: clarkji@u.washington.edu

[a]University of Washington, Department of Biological Structure, Seattle, WA 98195-7420, USA

[b]Benaroya Research Institute, 1201 9th Ave, Seattle, WA 98101-2795, USA

[c]University of Washington, Department of Biological Structure and Ophthalmology, Seattle, WA, 98195-7420, USA

Abstract

SPARC is a matricellular glycoprotein involved in regulation of extracellular matrix, growth factors, adhesion, and migration. SPARC-null mice have altered basement membranes and develop posterior sub-capsular cataracts with cell swelling and equatorial vacuoles. Exchange of fluid, nutrients, and waste products in the avascular lens is driven by a unique circulating ion current. In the absence of SPARC, increased circulation of fluid, ions, and small molecules led to increased fluorescein distribution *in vivo*, loss of resting membrane polarization, and altered distribution of small molecules. Microarray analysis of SPARC-null lenses showed changes in gene expression of ion channels and receptors, matrix and adhesion genes, cytoskeleton, immune response genes, and cell signaling molecules. Our results confirm the hypothesis that the regulation of SPARC on cell-capsular matrix interactions can increase the circulation of fluid and ions in the lens, and the phenotype in the SPARC-null mouse lens is the result of multiple intersecting functional pathways.

Keywords

SPARC; lens; circulation; cataract; matrix; capsule; electrophysiology; microarray

INTRODUCTION

SPARC (Secreted Protein Acidic and Rich in Cysteine, also known as BM-40 or osteonectin) is a matricellular glycoprotein that binds components of the extracellular matrix, affects certain growth factors, alters expression of matrix metalloproteinases, and has counter-adhesive and anti-angiogenic effects (Bornstein and Sage, 2002; Bradshaw and Sage, 2001; Brekken and Sage, 2001). In SPARC-null mice the composition, production, and structure of basement membranes and their corresponding functions in the lens are altered although growth and reproduction of the mice is normal. SPARC-null mice exhibit altered dermal basement membranes with decreased collagen I deposition and decreased tensile strength (Bradshaw et al., 2003), a diminished capacity to encapsulate tumors and implanted foreign bodies (Brekken et al., 2003; Puolakkainen et al., 2003), osteopenia with decreased bone formation (Delany et al., 2003; Machado do Reis et al., 2008), and lenticular cataracts with 100% penetrance

Corresponding Author John I. Clark, Box 357420, Seattle, WA 98195-7420, (206) 685-0950 phone, (206) 543-1524 fax.

(Gilmour et al., 1998; Norose et al., 1998). Recent studies of lens epithelial cells from SPARC-null mice linked posterior capsular opacity (PCO) to an epithelial mesenchymal transition (EMT) and found that SPARC can regulate cell-matrix interactions and inhibit PCO formation (Gotoh et al., 2007).

At one-month of age, mild cell swelling was observed at the lens equator in SPARC-null mice with a SPARC deletion in exon 4 on a C57Bl/6 background (Yan et al., 2002). By 3- to 4-months of age, the cell swelling progressed to a ring of large vacuoles around the equator of the lens. (Bassuk et al., 1999). Concomitantly, abnormal filopodia invaded the posterior lens capsule (Norose et al., 2000; Yan et al., 2003; Yan et al., 2002), and a posterior sub-capsular lens opacification was observed (Norose et al., 1998). Filopodial projections into the capsule increased in number and fiber cells failed to elongate or migrate toward the posterior pole, resulting in posterior displacement of the lens nucleus and eventual rupture of the posterior capsule by about 6-months of age (Bassuk et al., 1999; Gilmour et al., 1998; Norose et al., 1998). The opacification was slow and progressive during aging and became a full mature cataract at 4-6 months of age (figure 1). In another strain of SPARC-null mice with an exon 6 deletion on the 129/SvEv×MF1 background the onset was delayed until 6-9 months of age and was followed by a similar pattern of progression with rupture of the posterior capsule by 10-20 months (Gilmour et al., 1998).

Abnormal laminin and fibronectin distribution in the SPARC-null lens capsule correlated with the abnormal cell-matrix interactions between the capsular basement membrane and basal surfaces of epithelial and migrating fiber cells (Yan et al., 2005). The progressive penetration of filopodia into the abnormal lens capsule can account for the impaired fiber cell migration and elongation followed by the rupture of the posterior capsule. While the absence of SPARC in the capsule is consistent with impaired cell-capsule interactions, the relationship between SPARC and cell swelling and vacuole formation remains unexplained. We hypothesized a direct connection between SPARC and increased fluid circulation in the lens.

The lens employs an elegant microcirculatory system involving ion channels, aquaporins, and gap junctions in lieu of a vascular supply (see (Donaldson et al., 2001; Mathias et al., 2007; Mathias et al., 1997) for reviews). Lens fibers lose their nuclei and all organelles large enough to scatter light during maturation, but the lens still needs nutrients like glucose for anaerobic metabolism and glutathione for its antioxidant capacity to maintain transparency. A unique circulating sodium current creates an energy supply that drives the movement of water, nutrients, and metabolites into and out of the lens (figure 2). In brief, Na^+ ions enter the extracellular spaces between lens cells and move down the electrochemical gradient into fiber cells (which maintain a resting potential of approximately -70mV) through an unidentified Na^+ leak channel or gap junction hemichannel. Once in a fiber cell, Na^+ passes through gap junctions which are preferentially open along the equatorial plane, and is pumped out of lens epithelial cells by Na/K/ATPase which is concentrated in equatorial epithelial cells. The result is a symmetric, circulating sodium current in which Na^+ enters the lens through the anterior and posterior poles and exits near the equator. Other ion channels and transporters use the sodium current either directly or indirectly to move ions and nutrients against their concentration gradients. For example, transport of water, calcium, glutamate, and glucose are all dependent on the sodium current (Mathias et al., 2007) and lenses placed in a low-sodium medium quickly opacify (Tamiya and Delamere, 2006).

The near perfect symmetry required for a functional, transparent lens is created by the coordinated proliferation, migration, and elongation of fiber cells during lens growth. Symmetric circulation through the lens requires the symmetric distribution of ion channels, pumps, and transporters within a fiber cell which would suggest a functional correlation between the symmetry of circulation and fiber cell development. When fiber cell symmetry

was impaired, e.g. in fiber cells of SPARC-null mice which have difficulty migrating and elongating toward the posterior pole, it seems logical that lens circulation was impaired. The presence of cell swelling and equatorial vacuoles alone was an indication of increased circulation or transport in the lenses of SPARC-null mice. Further evidence was provided when it was shown that uptake of trypan blue dye, [^{3}H]-thymidine, or tracers increased in *ex vivo* lenses of SPARC-null mice relative to those from wild-type littermates (Yan et al., 2002). In this paper, we determined that the circulation of fluid, ions and small fluorescent molecules was abnormal in the absence of SPARC. Increased fluid led to equatorial vacuoles and increased fluorescein distribution *in vivo*, and changes in the distribution of ions and small molecules resulted in depolarized membrane resting voltage. Microarray analysis revealed changes in ion channels and transporters in addition to genes involved in matrix function, adhesion, cytoskeleton, immune response, and cell signaling, demonstrating that multiple intersecting pathways were altered by lack of SPARC.

MATERIALS AND METHODS

Mice

SPARC-null animals were generated by the lab of Dr. E. Helene Sage (Bassuk et al., 1999) and back-crossed with C57Bl/6 wild-type mice (Jackson Laboratory) for seven generations. Euthanasia was performed with CO_2 followed by cervical dislocation. Animals were housed and cared for by the University of Washington Department of Comparative Medicine. All protocols and procedures were approved by the University of Washington Institutional Animal Care and Use Committee.

Paraffin sectioning and vacuole stains

For Hematoxylin and Eosin or Alcian Blue stains: whole eyes were fixed in Methacarn (60% methanol, 30% chloroform, 10% acetic acid) for 4 hours at room temperature or at 4°C overnight followed by 3 washes in 70% ethanol. Eyes were mounted in paraffin blocks, cut into 15μm sections, and mounted on charged slides followed by staining. For Oil Red O stain: whole eyes were frozen in OCT at -80°C, cut into 15μm cryosections, and mounted on charged slides which were air dried for 30 minutes, fixed in 10% formalin for 5 minutes, and stained.

Slit lamp and fluorescein injection

Sodium Fluorescein (AK-Fluor 10%, Akorn) was injected intra-peritoneally at 0.6mg per gram mouse body mass into age- and sex-matched animals. Mouse eyes were examined by slit lamp *in vivo* as described previously (Seeberger et al., 2004) prior to injection and at selected intervals up to 48-hours post-injection. Briefly, the eyes of unanesthetized mice were dilated with a 1:1 mixture of 10% phenylephrine (Akorn) and 1% tropicamide (Bausch and Lomb) and animals were held gently in front of a slit lamp biomicroscope (Nikon FS2). Examinations were recorded by digital video and still images were captured from video using Adobe Premiere 6.0. A fluorescein excitation filter (480nm) was placed in front of the illumination source for part of the exam, followed by an emission filter (535nm) for incoming light.

Electrophysiology

Lenses were prepared for recording as described previously (Baldo and Mathias, 1992). Briefly, an “X” was cut into the posterior half of freshly enucleated eyes to create four flaps of tissue that were pinned to a sylgard dish filled with Tyrode’s solution (Tyrode’s salts (Sigma) with 1.2mM KCl and 5mM HEPES, pH 7.4). The retina and vitreous humor were removed to allow access to the lens. A glass microelectrode with 3-5 MΩ resistance made from a 1.5mm diameter capillary tube and back-filled with 2.5M potassium acetate was introduced into the posterior lens at a 35° angle and slowly driven toward the center of the lens. Resting membrane

potential voltages were recorded every ~50μm from just under the capsule to the center of the lens and averaged across the lens radius.

Laser Capture Microdissection

Freshly enucleated eyes from 4-week old littermate SPARC-null and wild-type mice were immediately mounted in Tissue-Tek O.C.T. (Sakura Finetek), frozen on dry ice, and stored at -80°C. Eyes were cut into 12μm sections using a Leica CM1850 cryostat at -17°C with disposable blades. Sections were mounted on Superfrost plus slides (VWR) and stored at -80° C for up to one week. Slides were stained and dehydrated as follows: 30 seconds in 70% ethanol, 30 seconds in water, 40 seconds in 0.5% Cressyl Violet stain, 10 dips in water, 30 seconds in 70% ethanol, 30 seconds in 95% ethanol, 2 × 1 minute in 100% ethanol, 10 dips in xylene, 5-60 minutes in xylene, 5 minutes drip dry in room air. Coplin jars were pre-treated with RNAse Zap (Ambion) and rinsed with 70% ethanol. All water was nuclease-free (Ambion).

Lens epithelial cells were captured from whole eye sections using the Arcturus PixCell 2e Laser Capture Microdissection (LCM) system and CapSure Macro LCM caps (Arcturus). Approximately 18 sections were captured on each cap and 72 sections total were captured per lens.

RNA extraction and Gene Chip Arrays

RNA was extracted from captured tissue using the RNeasy micro kit (Qiagen) and assayed for quality using the Bioanalyzer 2100 (Agilent). RNA integrity number (RIN) values ranged from 7.1-8.5. 19ng of RNA from each eye respectively underwent double-round amplification and fragmentation using the Ambion MessageAmp II aRNA amplification kit and the MessageAmp II-biotin enhanced amplification kits. 20μg of aRNA were used to make the target using the GeneChip hybridization, wash and stain kit (Affymetrix) and hybridized to Affymetrix GeneChip mouse genome 430 2.0 arrays. Microarray data was analyzed with GCOS (Affymetrix) and deposited in NCBI's Gene Expression Omnibus (Edgar et al., 2002) and is accessible through GEO Series accession number **GSE13402** (http://www.ncbi.nlm.nih.gov/geo/query/acc.cgi?acc=GSE13402). GeneSifter software (VizX Labs) was used to perform a pair-wise statistical analysis of the 3 wild-type and 4 SPARC-null lens gene expression arrays. Genes considered significant had a "present" quality call (meaning the expression level was high enough to be measured reliably), a p-value ≤ 0.05 when taking the mean expression level of the gene between the 3 wild-type or 4 SPARC-null lenses, and a ≥ 2.0-fold-change threshold which is often used as a standard cut-off in microarray analysis (Draghici, 2003).

Quantitative real time PCR

Lens capsules were removed from freshly enucleated eyes, blotted on filter paper, and placed immediately into RNAlater (Qiagen). The majority of lens epithelial cells remained attached to the lens capsule but the bulk of fiber cells were removed. Lens capsules were removed from RNAlater and total RNA was extracted using the RNeasy mini kit (Qiagen) protocol with Proteinase K digestion and DNAse digestion. RNA extracted from lens epithelium/capsules or LCM was transcribed into cDNA using the SuperScript III first strand synthesis kit (Invitrogen). PCR amplification was performed on an ABI 7900 HT real-time system (Applied Biosystems) using SYBR Green qPCR SuperMix (Invitrogen) for the genes C4b, Kcne1, Kng1, Serping1, and Socs3 (table 1). Mouse GAPDH was used for standardization. PCR was performed with 40 cycles of amplification following the suggested Invitrogen protocol: 50°C for 2 minutes, 95°C for 2 minutes, followed by 40 cycles of 95°C for 15 seconds and 60°C for 1 minute. TaqMan Gene Expression Assays (Applied Biosystems) were used to amplify the genes Adam23, Gria1, Gad1, Pcdh9, Slc1a1, Slc2a3, and Slc8a1 (table 2). A probe for mouse GAPDH labeled with Vic dye (Applied Biosystems) was used as the endogenous control. PCR

was performed on a Chromo4 Real-Time PCR detection system (Bio-Rad) with 40 cycles of amplification following the suggested ABI protocol: 50°C for 2 minutes, 95°C for 10 minutes, followed by 40 cycles of 95°C for 15 seconds and 60°C for 1 minute. Fold-change was calculated using the relative quantitation comparative C_t method (Wong and Medrano, 2005).

Glutamate immunohistochemistry

Mouse lenses were fixed, frozen, and sectioned as previously described (Jacobs et al., 2003). Briefly, lenses were fixed in 0.75% w/v paraformaldehyde and 0.1% glutaraldehyde for 24 hours followed by cryoprotection in sucrose and frozen in OCT. 10μm sections were cut at -18°C on a cryostat (Leica CM1850) and mounted on Superfrost plus slides (VWR). Sections were pre-treated with blocking solution (3% w/v BSA, 3% w/v fetal calf serum) to reduce nonspecific labeling and then labeled with polyclonal rabbit anti-glutamate (1:200; Chemicon) followed by secondary goat anti-rabbit AlexaFluor 488 (1:200) and WGA:AlexaFluor 550 (1:200). Sections were mounted in Vectashield (Vector Laboratories) and viewed using a confocal laser scanning microscope (Zeiss LSM 510). A z-series of image stacks were acquired and used to generate z-projections using NIH ImageJ and Adobe Photoshop.

RESULTS

Lens equatorial vacuole staining

In sections of SPARC-null lenses, swollen secondary fibers and prominent lens vesicles were observed at the equator and bow region (figure 3). Histological staining was used to evaluate the contents of the vacuoles for proteins and DNA using Hematoxylin & Eosin, carbohydrates using Alcian blue, and lipids using Oil Red O. In four-month-old lenses with obvious peripheral vacuoles on slit lamp examination, the staining of the vacuoles with the three dyes was negligible (figure 3) indicating that abnormal accumulation or aggregation of proteins, carbohydrates, or lipids had not caused the vacuoles in SPARC-null lenses. This observation suggested that the vacuoles were fluid-filled and may be related to increased fluid accumulation in the lens due to defective circulation in the absence of SPARC.

Fluorescein penetration following systemic intravenous injection

Fluid circulation in the lens was examined *in vivo* using a slit lamp equipped for fluorescence to study water-soluble fluorescein distribution in the eyes of sodium fluorescein-injected SPARC-null and wild-type mice (figure 4). Within a few minutes after systemic injection, fluorescein leaked from capillaries in the ciliary process into the aqueous humor. Penetration of fluorescein from the aqueous humor into the lens occurred slowly over a period of 12-18 hours until all systemic fluorescein was cleared from the circulation by renal excretion. Diffusion of fluorescein in the radial direction (from superficial to deep fiber cells) was much slower than diffusion of fluorescein within a single cell or to cells within the same layer (i.e. radial shell). This resulted in a complete “shell” or “ring” of fluorescein distribution encircling the lens at all time points even though fluorescein entered only from the anterior side of the lens. Fluorescein angiograms in SPARC-null mice did not show obvious retinal vessel leakage and it was concluded that fluorescein does not enter the vitreous humor in these animals.

At selected ages ranging from 1-3 months, fluorescein accumulation in the lenses of SPARC-null animals was both brighter and deeper than in wild-type lenses. Figure 4 shows two wild-type and two SPARC-null eyes, all two-months of age, prior to injection and at 24-hours post-injection. Note the mild anterior and posterior subcapsular opacity in the SPARC-null lenses (Figure 4C, D arrows). After 24-hours, the fluorescein penetrated deeper into the SPARC-null lenses than the wild-type lenses and was brighter in intensity (Figure 4G, H). Slit lamp imaging with fluorescein excitation and emission filters was used to distinguish fluorescein dye from light scattering (Figure 4I-P). In SPARC-null lenses, fluorescence imaging determined that

water-soluble fluorescein penetration increased or fluorescein clearance decreased, resulting in the increased accumulation observed at 24-hours post-injection. *In vivo*, the penetration into and diffusion out of the lens fibers in the cortex was altered in the absence of SPARC indicating the importance of SPARC for normal fluid circulation.

Lens Electrophysiology

The intracellular resting voltage of lens cells was measured *ex vivo* in lenses from 4-month-old SPARC-null and wild-type mice in order to test ion circulation. The SPARC-null lens had posterior subcapsular opacity but no obvious vacuoles. A recording electrode was driven from the posterior surface of the lens just under the capsule to the center of the lens in 50-100 μm increments and the intracellular resting voltage was measured at each step. The intracellular resting potential in wild-type mouse fiber cells had a mean value of -61.7 ± 1.84mV (figure 5). The resting potential in the SPARC-null lens was depolarized compared to the wild-type lens with a mean value of -35.9 ± 6.21mV which may indicate a change in ion channel distribution or function leading to impaired lens circulation. The electrophysiology data was consistent with partial loss of membrane polarity due to abnormal ion circulation in the absence of SPARC.

Gene Expression

Microarray analysis was used to compare gene expression levels in the lens epithelia of 4-week old SPARC-null (n=4) vs. wild-type (n=3) littermates. At four-weeks of age, the transparency of SPARC-null lenses observed in a slit lamp examination was accompanied by subtle cell swelling with a few protrusions from the lens epithelium into the capsule observed in histological sections. It was expected that analyzing the lenses in young SPARC-null animals would identify the earliest primary changes in gene expression in the absence of secondary modifications resulting from reactions to opacification and lens damage. The lens epithelium was isolated from the lens fiber cells beneath using laser capture microdissection in order to reduce “noise” in the array results by comparing gene expression from only one, transcriptionally-active cell-type.

Microarray analysis generated a list of 183 significantly changed genes with greater than 2-fold change in expression, of which 152 were up-regulated and 31 down-regulated in the SPARC-null lens samples (table 3). 54 genes were unknown ESTs. The array contained two spots for the SPARC gene which were calculated to be 1166-fold and 802-fold higher in the wild-type than the SPARC-null samples, confirming that those lenses were from null animals. Raw data and a complete gene list are available from NCBI GEO (series accession number **GSE13402**). The expression levels of eleven genes were tested using quantitative RT-PCR (table 3). While there were small differences between microarray and qRT-PCR, approximately three-quarters of the genes tested had significantly different gene expression in both arrays and PCR and all but one of the genes tested were consistently up- or down-regulated by both methods of testing gene expression. Inconsistency between individual array and qRT-PCR results confirmed the importance of categorization of the 129 altered genes by functional gene ontology. In lenses of SPARC-null mice, altered expression was observed for 23 ion channel and membrane receptor genes which were 18% of all significantly changed genes, 10 matrix/adhesion molecule genes (8%), 10 genes for cytoskeletal proteins (8%), 6 immune response genes (5%), and 5 cell signaling genes (4%) (table 3).

In the absence of SPARC, 13 cation channels had altered expression. Six potassium channels, one potassium channel regulator, three calcium channels, two sodium channels, and one less selective cation transporter were altered and were hypothesized to be important for maintenance of the circulating ion current of the lens. The remaining 10 genes listed in the “ion channels and receptors” category (table 3) related to the small molecules glucose, glutamate,

GABA, and glycine which have been reported to be important for function of the normal lens. The list included one glutamate transporter and four receptors; a GABA transporter, a GABA receptor, and an enzyme that converts glutamic acid to GABA; two glucose transporters; and one glycine receptor. The observed changes in the expression of receptor and transporter messages were consistent with the importance of SPARC regulation of matrix-cell interactions in the circulation of ions, fluid, and small molecules.

The next category of gene expression changes related to matrix and adhesion which are functions commonly associated with SPARC. This category included structural components of the extracellular matrix like collagen I and the small proteoglycan fibromodulin, and many genes associated with cellular adhesion including thrombospondin 2 (a matricellular glycoprotein in the same family as SPARC), cadherins 6 and 10, protocadherins 9 and 19, a disintegrin (Adam23), and a lectin (Lgals9). Cytoskeletal gene changes included 4 intermediate filaments, 5 genes involved in microtubule regulation, and one gene involved in actin regulation. The immune response category contained 6 genes, all up-regulated and all associated with the innate immune system, specifically with inflammation and cytokines. These gene products function to activate the inflammatory cascade (C4b, Kininogen) or inhibit/resolve inflammation (Socs3, Serping1, Pros1, and Rtn4rl2). Genes involved in GTP-dependent cell signaling cascades also showed altered expression. These included GEFs (guanine nucleotide exchange factors) which activate Ras and Rho family GTPases and GAPs (GTPase activating proteins) which inhibit GTPases. Two other notable genes up-regulated in the SPARC-null lens are transglutaminase 2C which is associated with protein aggregation and cataract, and DnajC1, a member of the chaperonin family that protects against protein unfolding and aggregation. In summary, altered expression of matrix and adhesion proteins was observed as expected. Changes were observed in cytoskeletal proteins, which may relate to the altered migration and elongation of fiber cells in SPARC-null lenses; inflammatory genes which are associated with the altered wound healing response in SPARC-null mice; and genes involved in cell signaling cascades which could result in changes in multiple downstream intersecting pathways. The results of the microarrays confirm the importance of the cell-matrix interactions controlled by the matricellular protein, SPARC, on downstream gene expression.

Glutamate immunohistochemistry

In microarray data of SPARC-null lenses, four glutamate receptors were up-regulated and one glutamate transporter was down-regulated, emphasizing the importance of glutamate receptors and transporters in lenses from SPARC-null mice. Lenses from 4-week-old wild-type and SPARC-null littermate animals were cryosectioned and stained with an antibody to glutamate (figure 6). In the wild-type lenses, abundant glutamate staining was observed in the lens epithelium with patchy staining in the outer cortex and no staining in the lens capsule. In contrast, the distribution of glutamate in the SPARC-null lens decreased in the lens epithelium and increased in the lens capsule. Altered glutamate distribution in the SPARC-null lens is consistent with the changes in glutamate transporter and receptor gene expression levels and also indicative of a more global change in the circulation of small molecules that could account for the observations in SPARC-null mice.

DISCUSSION

Our results established that the regulation of the cell-matrix interactions between lens epithelium and capsule can influence the unique circulation of fluid and ions in the lens and alter gene expression in lens epithelial cells. In the absence of SPARC, changes in the distribution of water, solutes, and small molecules in lens fiber cells accounted for fluid-filled vacuole formation, altered fluorescein distribution, electrophysiological changes, and altered levels of glutamate observed in the lenses of SPARC-null mice. Microarray analysis identified

alterations in the expression of mRNA for ion channels and receptors, matrix components, adhesion molecules, cytoskeletal proteins, immune response, and cell signaling pathways, demonstrating that multiple intersecting pathways were altered by the loss of matrix-cell interactions regulated by SPARC.

The equatorial distribution of lens vacuoles and the distribution of fluorescein in lenses of living mice were a measure of fluid accumulation in the lens, caused by insufficient regulation of fluid entry or outflow. Circulation of water in the lens is osmotically driven by the movement of solutes. While water must pass through aquaporin channels to cross the cell membrane, no changes in aquaporin genes were observed in microarray analysis and it is assumed that aquaporin expression is normal in SPARC-null mice. It is hypothesized that lens circulation is driven mainly by the sodium current (Mathias et al., 2007). As summarized above and in figure 2, sodium enters the anterior and posterior poles of the lens through extracellular spaces and leaks into lens fiber cells through an unidentified sodium leak channel. Intracellular sodium can exchange freely between fiber cells through gap junctions. Excess sodium is pumped out of the lens by Na/K/ATPase channels at the lens equator and expression of these pumps was found to be unchanged in the SPARC-null lens. Fluid and small molecules like glucose follow a similar circulation, ultimately driven by the sodium current. Thus, the symmetric inflow of solutes and water into the lens occurs at the anterior and posterior poles and the outflow occurs at the equator. In the absence of regulation of cell-matrix interactions by SPARC, the normal flow patterns were disrupted and fluid accumulated in the lens.

It is well established that the interactions between lens cells and the capsular matrix are vital for lens growth and development; human lens epithelial cells can survive and proliferate on the capsule in serum-free media (Al-Ghoul et al., 2003; Danysh and Duncan, 2008; Wormstone et al., 1997). *In vitro* interactions between cells and their underlying matrix can alter the expression and function of ion channels (Asem et al., 2002; Qin et al., 2002; Smith et al., 1998; Taranta et al., 2000; Vag et al., 2007). To our knowledge these are the first experimental results demonstrating a relationship between cell-matrix interactions in the lens and the activity of ion channels and pumps that regulate solute and fluid circulation. The analysis of mRNA using microarrays suggested that a variety of cation channels including sodium, potassium, and calcium pumps had abnormal expression. Altered intracellular levels of these ions could alter many important cellular processes including the function of ion exchange channels like Na/K/ATPase pumps, downstream signaling cascades, and the electrophysiological properties across the cell membrane, as was observed in SPARC-null mice. Indeed, the normal human aging cataract has been correlated with an increase in lens permeability to Na^+, K^+, and Ca^{2+} (Duncan et al., 1989).

In lens, the pump-leak mechanism that maintains the resting membrane potential is the result of potassium and sodium leak currents (Mathias et al., 2007). Analysis of the resting voltage of SPARC-null lens fibers found intracellular depolarization relative to the wild-type. In the lenses of SPARC-null mice, microarray analysis of the lens epithelium found an increase in the expression of Nalcn, a non-selective sodium leak channel recently shown to be responsible for resting potential in mouse hippocampus (Lu et al., 2007). If Nalcn is the unidentified sodium-leak channel responsible for resting potential in the lens and Nalcn channels were up-regulated, the resting voltage would become less negative, i.e. move away from the potassium equilibrium potential and toward the sodium equilibrium potential, as was observed in the SPARC-null lens.

While the presence in lens of ion channels and neurotransmitters usually associated with neurons may seem surprising, numerous literature references show the presence and importance of these molecules in the function of the crystalline lens. For example, two of the calcium channels found to be affected by lack of SPARC are Slc8a1 and Ryr2 which are

reported to maintain normal transparent structure (Paul et al., 2003; Tamiya and Delamere, 2006), and the links between calcium balance and cataract are well established (Duncan and Collison, 2002; Duncan and Jacob, 1984; Duncan and Wormstone, 1999). Given recent studies of lens opacification in neurodegenerative disease, the previously unrecognized link between the lens and the nervous system suggests a logical connection between the function of ion channels in both tissues (Goldstein et al., 2003; Muchowski et al., 2008).

In the microarrays, the expression of genes associated with matrix, adhesion, filaments, and the immune response were altered. One of the down-regulated matrix genes, thrombospondin 2, is a member of the matricellular protein family found in the lens epithelium. Knocking out thrombospondin 2 in addition to SPARC potentiates the accelerated dermal wound healing response observed in single-null mice, indicating the importance of cell-matrix interactions (Hiscott et al., 2006; Puolakkainen et al., 2005). The relationship between SPARC and type I collagen was established by a previous report showing decreased dermal protein levels of type I collagen in SPARC-null mice (Bradshaw et al., 2003) and further confirmed by array studies showing decreased type I collagen expression in the SPARC-null lens. Altered expression of filament genes in the SPARC-null lens could relate to the effects of SPARC on lens fiber migration and elongation. The abnormal expression of matrix, adhesion, and filament genes among other cataractous changes may cause a type of “wound healing response” in lens cells leading to the altered expression of inflammatory genes observed in the SPARC null lens.

In a previous microarray analysis of gene expression in the SPARC-null mouse lens, changes in globins and other genes were described (Mansergh et al., 2004). Altered expression of globin genes was not observed in our study although Serping1, Transglutaminase 2C, type 1 collagen, and members of the complement cascade were altered in both Mansergh et al. and the current study. Differences between microarray results are expected when there are major differences in methodology, animal age, genetic background, and array platform among other factors. In our study, SPARC-null animals were 4-weeks-old which was much younger than the Mansergh study. Our goal was to identify early, causative alterations in gene expression well before secondary changes resulting from cellular damage in the SPARC-null animals were present. The microarray results we report are consistent with the observed phenotype and establish new relationships between electrophysiological and cell-matrix interactions that have functional significance.

In separate studies a striking example of interactions between matrix, ion channels, and cytoskeleton was observed using a line of transgenic mice in which Rho GTPase function was inactivated in the lens (Maddala et al., 2004). It has been hypothesized that small GTPases play a critical role in lens growth and function through downstream signaling cascades that target many cellular processes including the actin cytoskeleton, cell-cell adhesion, transcription, and apoptosis (Maddala et al., 2008; Mitchell et al., 2007; Rao et al., 2002; Xie et al., 2006). Animals lacking rho in the lens had grossly swollen and disorganized lenses with rupture of the posterior capsule and large equatorial and anterior vacuoles, similar to the phenotype in SPARC-null mouse lenses although with an earlier onset. Microarray analysis of rho functional knockout lenses revealed changes in genes involved in matrix and ion channels as well as impaired cytoskeletal organization based on immunohistochemistry. Interestingly, altered expression of five G-protein cascade regulating genes were observed in SPARC-null lenses, indicating that the GTPases may play a role downstream of SPARC. This relationship could account for interactions between SPARC and integrin-linked kinase (ILK)(Barker et al., 2005), a multi domain focal adhesion protein involved in signal transmission which can act on many downstream effectors and pathways including the small G-proteins (see (Boulter and Van Obberghen-Schilling, 2006) for review). Lack of SPARC activating ILK at the plasma membrane would disrupt multiple downstream pathways important for lens growth and

development and lead to the observed changes in adhesion, elongation and migration, ion channels, and cytoskeletal genes.

The current study established a relationship between the matricellular function of SPARC in lens and the regulation of fluid balance, ions and small molecules involving the cytoskeleton, and signaling pathways. What has become obvious from the many studies of SPARC is that matricellular proteins regulate a multifactorial system responsible for disruptive phenotypes produced by multiple intersecting functional pathways.

Acknowledgments

The authors would like to thank Mr. Hidayat Djajadi for his work on immunohistochemistry, Ms. Crystal Rawling for her assistance with qPCR, and the laboratory of Dr. Peter Detwiler for their assistance with electrophysiology. Support was generously provided by NEI EY04542 (JIC) and EY07031 (TMG).

References

Al-Ghoul KJ, Kuszak JR, Lu JY, Owens MJ. Morphology and organization of posterior fiber ends during migration. Mol Vis 2003;9:119–28. [PubMed: 12707642]

Asem EK, Qin W, Rane SG. Effect of basal lamina of ovarian follicle on T- and L-type Ca(2+) currents in differentiated granulosa cells. Am J Physiol Endocrinol Metab 2002;282:E184–96. [PubMed: 11739100]

Baldo GJ, Mathias RT. Spatial variations in membrane properties in the intact rat lens. Biophys J 1992;63:518–29. [PubMed: 1420894]

Barker TH, Baneyx G, Cardo-Vila M, Workman GA, Weaver M, Menon PM, Dedhar S, Rempel SA, Arap W, Pasqualini R, Vogel V, Sage EH. SPARC regulates extracellular matrix organization through its modulation of integrin-linked kinase activity. J Biol Chem 2005;280:36483–93. [PubMed: 16115889]

Bassuk JA, Birkebak T, Rothmier JD, Clark JM, Bradshaw A, Muchowski PJ, Howe CC, Clark JI, Sage EH. Disruption of the Sparc locus in mice alters the differentiation of lenticular epithelial cells and leads to cataract formation. Exp Eye Res 1999;68:321–31. [PubMed: 10079140]

Bornstein P, Sage EH. Matricellular proteins: extracellular modulators of cell function. Curr Opin Cell Biol 2002;14:608–16. [PubMed: 12231357]

Boulter E, Van Obberghen-Schilling E. Integrin-linked kinase and its partners: a modular platform regulating cell-matrix adhesion dynamics and cytoskeletal organization. Eur J Cell Biol 2006;85:255–63. [PubMed: 16546570]

Bradshaw AD, Puolakkainen P, Dasgupta J, Davidson JM, Wight TN, Helene Sage E. SPARC-null mice display abnormalities in the dermis characterized by decreased collagen fibril diameter and reduced tensile strength. J Invest Dermatol 2003;120:949–55. [PubMed: 12787119]

Bradshaw AD, Sage EH. SPARC, a matricellular protein that functions in cellular differentiation and tissue response to injury. J Clin Invest 2001;107:1049–54. [PubMed: 11342565]

Brekken RA, Puolakkainen P, Graves DC, Workman G, Lubkin SR, Sage EH. Enhanced growth of tumors in SPARC null mice is associated with changes in the ECM. J Clin Invest 2003;111:487–95. [PubMed: 12588887]

Brekken RA, Sage EH. SPARC, a matricellular protein: at the crossroads of cell-matrix communication. Matrix Biol 2001;19:816–27. [PubMed: 11223341]

Danysh BP, Duncan MK. The lens capsule. Exp Eye Res. 2008

Delany AM, Kalajzic I, Bradshaw AD, Sage EH, Canalis E. Osteonectin-null mutation compromises osteoblast formation, maturation, and survival. Endocrinology 2003;144:2588–96. [PubMed: 12746322]

Donaldson P, Kistler J, Mathias RT. Molecular solutions to mammalian lens transparency. News Physiol Sci 2001;16:118–23. [PubMed: 11443230]

Draghici, S. Data Analysis Tools for DNA Microarrays. Chapman & Hall/CRC; Boca Raton, FL: 2003.

Duncan G, Collison DJ. Calcium signalling in ocular tissues: functional activity of G-protein and tyrosine-kinase coupled receptors. Exp Eye Res 2002;75:377–89. [PubMed: 12387785]

Duncan G, Hightower KR, Gandolfi SA, Tomlinson J, Maraini G. Human lens membrane cation permeability increases with age. Invest Ophthalmol Vis Sci 1989;30:1855–9. [PubMed: 2759800]

Duncan G, Jacob TJ. Calcium and the physiology of cataract. Ciba Found Symp 1984;106:132–52. [PubMed: 6096095]

Duncan G, Wormstone IM. Calcium cell signalling and cataract: role of the endoplasmic reticulum. Eye 1999;13(Pt 3b):480–3. [PubMed: 10627828]

Edgar R, Domrachev M, Lash AE. Gene Expression Omnibus: NCBI gene expression and hybridization array data repository. Nucleic Acids Res 2002;30:207–10. [PubMed: 11752295]

Gilmour DT, Lyon GJ, Carlton MB, Sanes JR, Cunningham JM, Anderson JR, Hogan BL, Evans MJ, Colledge WH. Mice deficient for the secreted glycoprotein SPARC/osteonectin/BM40 develop normally but show severe age-onset cataract formation and disruption of the lens. Embo J 1998;17:1860–70. [PubMed: 9524110]

Goldstein LE, Muffat JA, Cherny RA, Moir RD, Ericsson MH, Huang X, Mavros C, Coccia JA, Faget KY, Fitch KA, Masters CL, Tanzi RE, Chylack LT Jr, Bush AI. Cytosolic beta-amyloid deposition and supranuclear cataracts in lenses from people with Alzheimer's disease. Lancet 2003;361:1258–65. [PubMed: 12699953]

Gotoh N, Perdue NR, Matsushima H, Sage EH, Yan Q, Clark JI. An in vitro model of posterior capsular opacity: SPARC and TGF-beta2 minimize epithelial-to-mesenchymal transition in lens epithelium. Invest Ophthalmol Vis Sci 2007;48:4679–87. [PubMed: 17898292]

Hiscott P, Paraoan L, Choudhary A, Ordonez JL, Al-Khaier A, Armstrong DJ. Thrombospondin 1, thrombospondin 2 and the eye. Prog Retin Eye Res 2006;25:1–18. [PubMed: 15996506]

Jacobs MD, Donaldson PJ, Cannell MB, Soeller C. Resolving morphology and antibody labeling over large distances in tissue sections. Microsc Res Tech 2003;62:83–91. [PubMed: 12938120]

Lu B, Su Y, Das S, Liu J, Xia J, Ren D. The neuronal channel NALCN contributes resting sodium permeability and is required for normal respiratory rhythm. Cell 2007;129:371–83. [PubMed: 17448995]

Machado do Reis L, Kessler CB, Adams DJ, Lorenzo J, Jorgetti V, Delany AM. Accentuated osteoclastic response to parathyroid hormone undermines bone mass acquisition in osteonectin-null mice. Bone 2008;43:264–73. [PubMed: 18499553]

Maddala R, Deng PF, Costello JM, Wawrousek EF, Zigler JS, Rao VP. Impaired cytoskeletal organization and membrane integrity in lens fibers of a Rho GTPase functional knockout transgenic mouse. Lab Invest 2004;84:679–92. [PubMed: 15094715]

Maddala R, Reneker LW, Pendurthi B, Rao PV. Rho GDP dissociation inhibitor-mediated disruption of Rho GTPase activity impairs lens fiber cell migration, elongation and survival. Dev Biol 2008;315:217–31. [PubMed: 18234179]

Mansergh FC, Wride MA, Walker VE, Adams S, Hunter SM, Evans MJ. Gene expression changes during cataract progression in Sparc null mice: differential regulation of mouse globins in the lens. Mol Vis 2004;10:490–511. [PubMed: 15303089]

Mathias RT, Kistler J, Donaldson P. The lens circulation. J Membr Biol 2007;216:1–16. [PubMed: 17568975]

Mathias RT, Rae JL, Baldo GJ. Physiological properties of the normal lens. Physiol Rev 1997;77:21–50. [PubMed: 9016299]

Mitchell DC, Bryan BA, Liu JP, Liu WB, Zhang L, Qu J, Zhou X, Liu M, Li DW. Developmental expression of three small GTPases in the mouse eye. Mol Vis 2007;13:1144–53. [PubMed: 17653061]

Muchowski PJ, Ramsden R, Nguyen Q, Arnett EE, Greiling TM, Anderson SK, Clark JI. Noninvasive measurement of protein aggregation by mutant huntingtin fragments or alpha-synuclein in the lens. J Biol Chem 2008;283:6330–6. [PubMed: 18167346]

Norose K, Clark JI, Syed NA, Basu A, Heber-Katz E, Sage EH, Howe CC. SPARC deficiency leads to early-onset cataractogenesis. Invest Ophthalmol Vis Sci 1998;39:2674–80. [PubMed: 9856777]

Norose K, Lo WK, Clark JI, Sage EH, Howe CC. Lenses of SPARC-null mice exhibit an abnormal cell surface-basement membrane interface. Exp Eye Res 2000;71:295–307. [PubMed: 10973738]

Paul M, Schulze-Bahr E, Breithardt G, Wichter T. Genetics of arrhythmogenic right ventricular cardiomyopathy--status quo and future perspectives. Z Kardiol 2003;92:128–36. [PubMed: 12596074]

Puolakkainen P, Bradshaw AD, Kyriakides TR, Reed M, Brekken R, Wight T, Bornstein P, Ratner B, Sage EH. Compromised production of extracellular matrix in mice lacking secreted protein, acidic and rich in cysteine (SPARC) leads to a reduced foreign body reaction to implanted biomaterials. Am J Pathol 2003;162:627–35. [PubMed: 12547720]

Puolakkainen PA, Bradshaw AD, Brekken RA, Reed MJ, Kyriakides T, Funk SE, Gooden MD, Vernon RB, Wight TN, Bornstein P, Sage EH. SPARC-thrombospondin-2-double-null mice exhibit enhanced cutaneous wound healing and increased fibrovascular invasion of subcutaneous polyvinyl alcohol sponges. J Histochem Cytochem 2005;53:571–81. [PubMed: 15872050]

Qin W, Rane SG, Asem EK. Basal lamina of ovarian follicle regulates an inward Cl(-) current in differentiated granulosa cells. Am J Physiol Cell Physiol 2002;282:C34–48. [PubMed: 11742796]

Rao V, Wawrousek E, Tamm ER, Zigler S Jr. Rho GTPase inactivation impairs lens growth and integrity. Lab Invest 2002;82:231–9. [PubMed: 11850536]

Seeberger TM, Matsumoto Y, Alizadeh A, Fitzgerald PG, Clark JI. Digital image capture and quantification of subtle lens opacities in rodents. J Biomed Opt 2004;9:116–20. [PubMed: 14715062]

Smith P, Rhodes NP, Shortland AP, Fraser SP, Djamgoz MB, Ke Y, Foster CS. Sodium channel protein expression enhances the invasiveness of rat and human prostate cancer cells. FEBS Lett 1998;423:19–24. [PubMed: 9506834]

Tamiya S, Delamere NA. The influence of sodium-calcium exchange inhibitors on rabbit lens ion balance and transparency. Exp Eye Res 2006;83:1089–95. [PubMed: 16839544]

Taranta A, Teti A, Stefanini M, D'Agostino A. Immediate cell signal induced by laminin in rat sertoli cells. Matrix Biol 2000;19:11–8. [PubMed: 10686421]

Vag J, Byrne EM, Hughes DH, Hoffman M, Ambudkar I, Maguire P, O'Connell BC. Morphological and functional differentiation of HSG cells: role of extracellular matrix and trpc 1. J Cell Physiol 2007;212:416–23. [PubMed: 17348017]

Wong ML, Medrano JF. Real-time PCR for mRNA quantitation. Biotechniques 2005;39:75–85. [PubMed: 16060372]

Wormstone IM, Liu CS, Rakic JM, Marcantonio JM, Vrensen GF, Duncan G. Human lens epithelial cell proliferation in a protein-free medium. Invest Ophthalmol Vis Sci 1997;38:396–404. [PubMed: 9040473]

Xie L, Overbeek PA, Reneker LW. Ras signaling is essential for lens cell proliferation and lens growth during development. Dev Biol 2006;298:403–14. [PubMed: 16889766]

Yan Q, Blake D, Clark JI, Sage EH. Expression of the matricellular protein SPARC in murine lens: SPARC is necessary for the structural integrity of the capsular basement membrane. J Histochem Cytochem 2003;51:503–11. [PubMed: 12642629]

Yan Q, Clark JI, Wight TN, Sage EH. Alterations in the lens capsule contribute to cataractogenesis in SPARC-null mice. J Cell Sci 2002;115:2747–56. [PubMed: 12077365]

Yan Q, Perdue N, Blake D, Sage EH. Absence of SPARC in murine lens epithelium leads to increased deposition of laminin-1 in lens capsule. Invest Ophthalmol Vis Sci 2005;46:4652–60. [PubMed: 16303962]

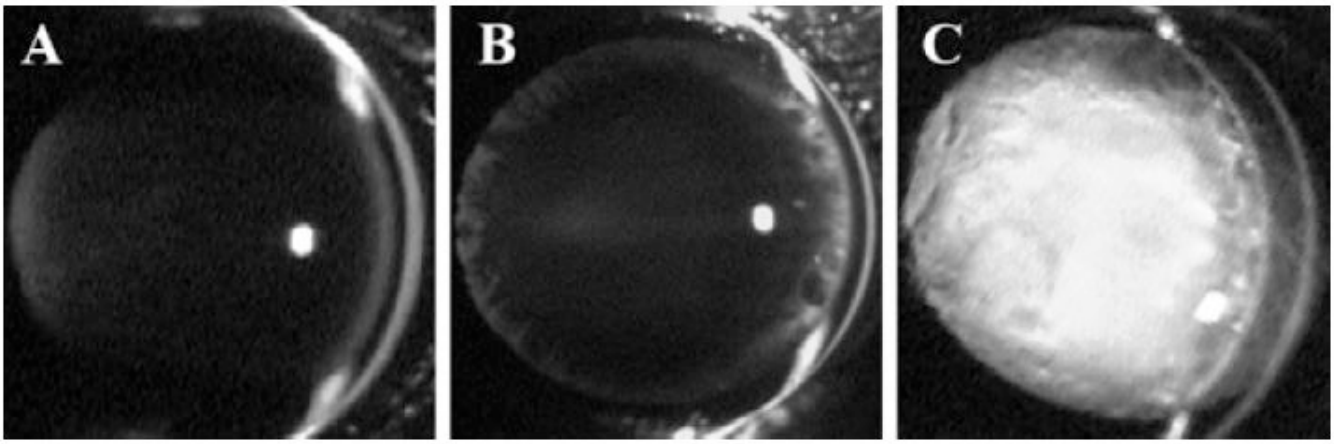

Figure 1.

Slit lamp images of living, unanesthetized SPARC-null mouse eyes. A vertical slit of light illuminates the eye from the right side of the image. The cornea and anterior lens epithelium/capsule are visible as bright white arcs while the anterior chamber and lens are dark, i.e. do not scatter light, in a normal eye. (A) At 1.5-months, a minor posterior sub-capsular opacity was observed in the lenses of SPARC-null mice. (B) At 4-months, large vacuoles were observed at the equator of the SPARC-null lens. (C) By 6-months, the SPARC-null lens was completely opaque. Deletion of the SPARC gene results in slow progressive opacification which includes posterior sub-capsular opacity, cell swelling, and equatorial vacuoles prior to full mature cataract.

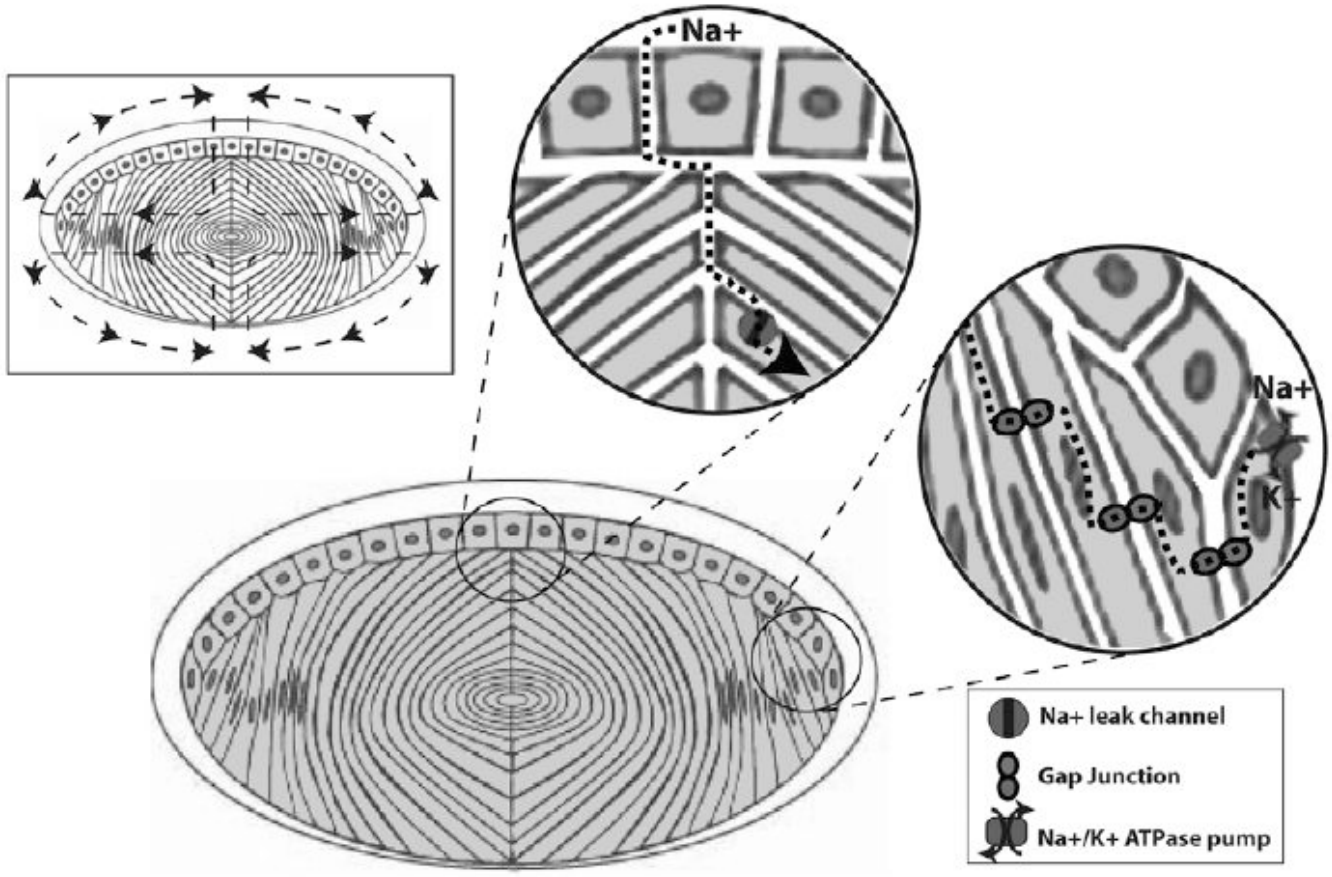

Figure 2.

Lens circulation. The central diagram represents a sagittal section of the lens epithelium and differentiating fibers surrounded by the lens capsule, a basement membrane which is thicker anteriorly than posteriorly. The symmetric circulation of sodium through the lens is presented in the rectangular inset (upper left). Sodium enters the lens mainly at the anterior and posterior poles and is pumped out of the lens at the equator via sodium/potassium ATPase pumps, as indicated by the direction of the arrows. At the anterior pole of the lens, sodium diffuses into the extracellular spaces and then enters a lens fiber cell through a sodium leak channel (top circular inset). At the lens equator sodium diffuses freely within fiber cells and between adjacent fibers through gap junctions until it is pumped out by equatorial cells in exchange for potassium (right circular inset). Malfunction of channels and pumps in the lens could lead to impaired circulation of sodium in addition to other ions, fluid, and small molecules. As a matricellular protein, SPARC regulates matrix-cell interactions that could influence channel and pump function leading to impaired circulation.

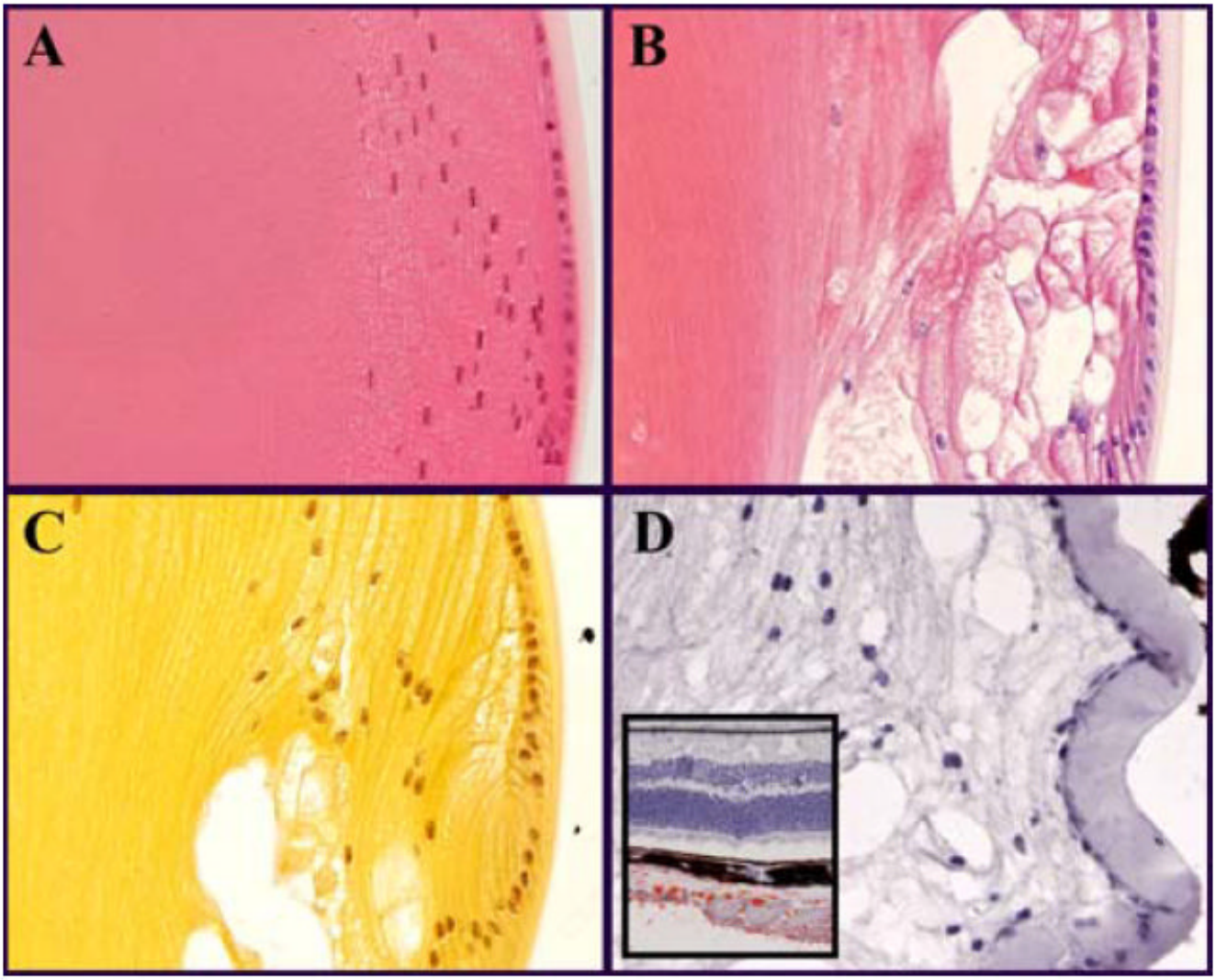

Figure 3.

Histological staining of the bow region at the equator of a 4-month-old lens. Sagittal section; anterior is oriented up. H&E stained sections of (A) WT and (B) SPARC-null lenses. Proteins stain pink and DNA stains violet. The large vacuoles in B appear to be empty and are surrounded by swollen cells. (C) Alcian blue with hematoxylin stained SPARC-null lens in which carbohydrates stain yellow. As with H&E alone, vacuoles do not stain. (D) Oil red O with hematoxylin stained lens in which lipids stain red. No lipid staining was observed in the lens while prominent red staining was observed in the sclera near the optic nerve entry (D, inset). Vacuoles at the SPARC-null lens periphery were not filled with proteins, carbohydrates, or lipids suggesting that abnormal fluid transport accounts for the cell swelling and vacuole formation in the absence of SPARC.

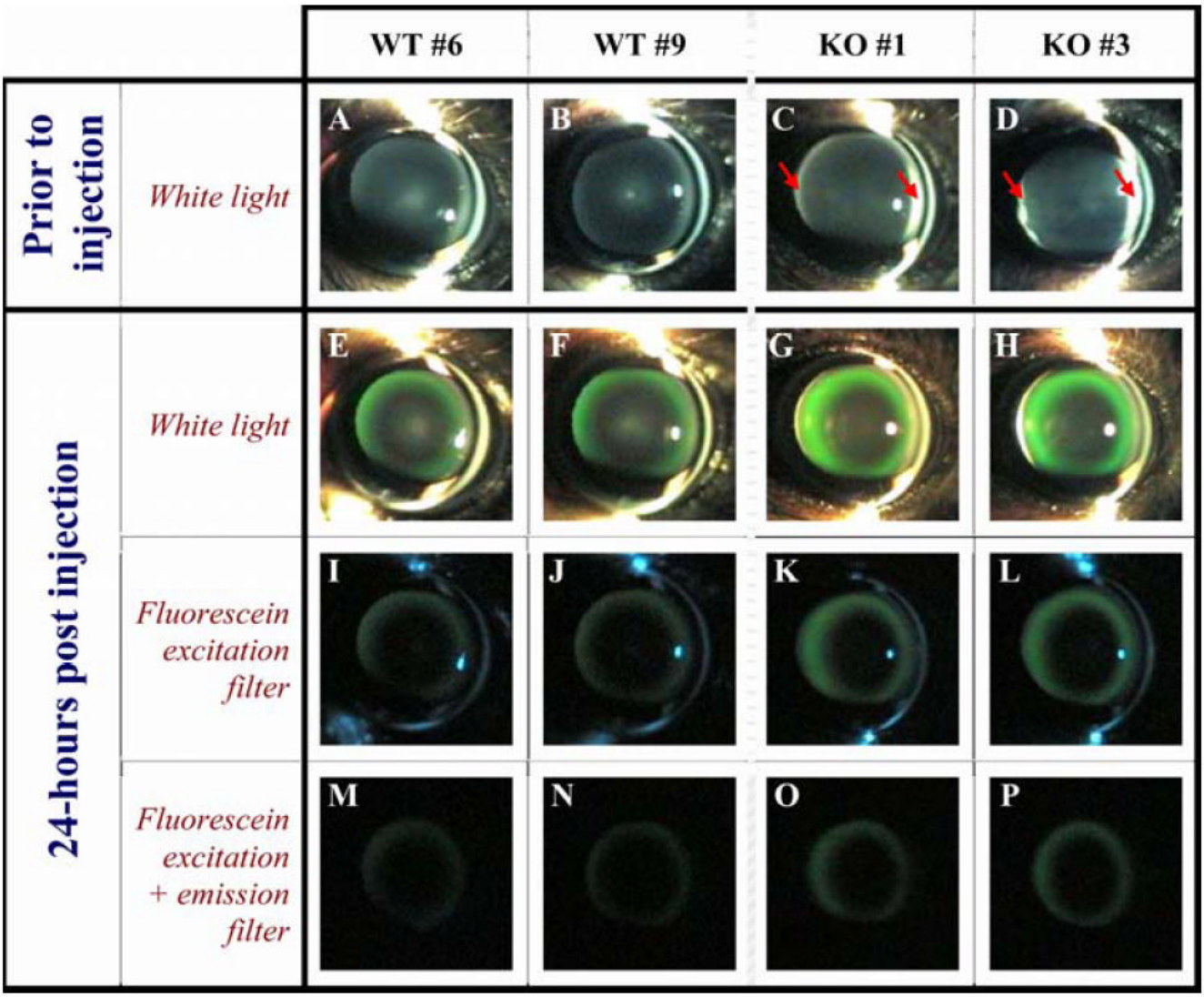

Figure 4.

Slit lamp views of fluorescein in the lens. The eyes of two wild-type (WT) and two SPARC-null mice (KO), (2-months-old) are shown in the 4 columns. The first row of images (A-D) contains slit lamp images of eyes prior to injection of fluorescein. Note the anterior and posterior subcapsular opacity in the SPARC-null lenses (red arrows). The second row (E-H) contains eyes 24-hours post-injection with white light illumination. All lenses contain fluorescein. In the SPARC-null lenses the fluorescein penetration is deeper and the fluorescence more intense than in wild-type lenses. When the green image channel is digitally isolated for quantification of fluorescence accumulation in the lens, the SPARC-null images have approximately 1.7-fold more pixel intensity in the lens than the wild-type images. The 3rd row (I-L) shows the same eyes with a fluorescein excitation filter and the 4th row (M-P) shows images with both fluorescein excitation and emission filters to help differentiate fluorescein from background excitation. The increased accumulation of water-soluble fluorescein indicates a change in fluid circulation in the SPARC-null lens.

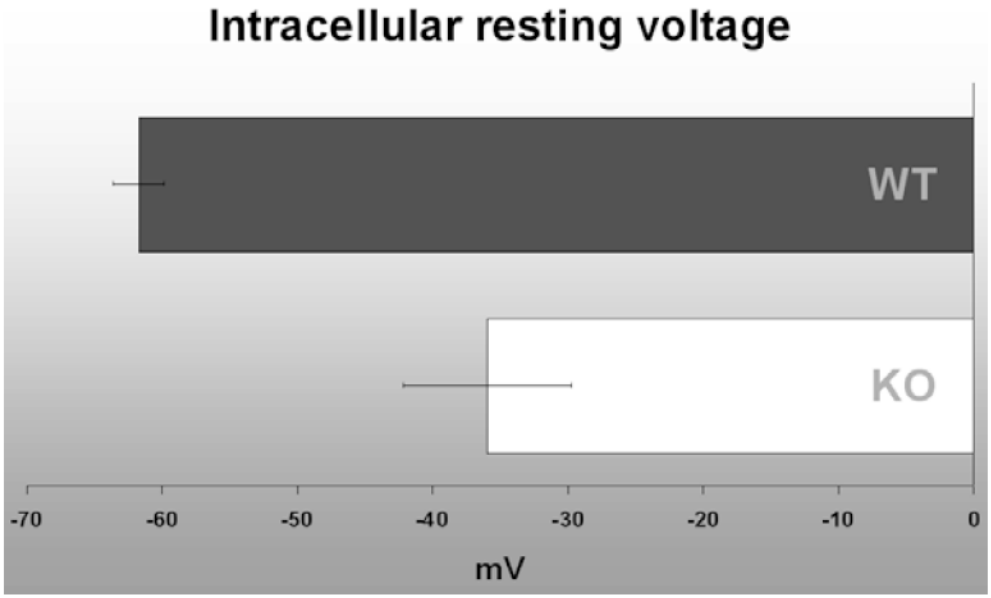

Figure 5.

Intracellular resting potential measured in 4-week-old SPARC-null and wild-type lenses. The intracellular resting potential in wild-type mouse fiber cells had a mean value of -61.7 ± 1.84mV. The resting potential in the SPARC-null lens was depolarized compared to the wild-type lens with a mean value of -35.9 ± 6.21mV. The change in electrophysiological properties is consistent with impaired ion circulation leading to a partial loss of membrane polarity in the absence of SPARC.

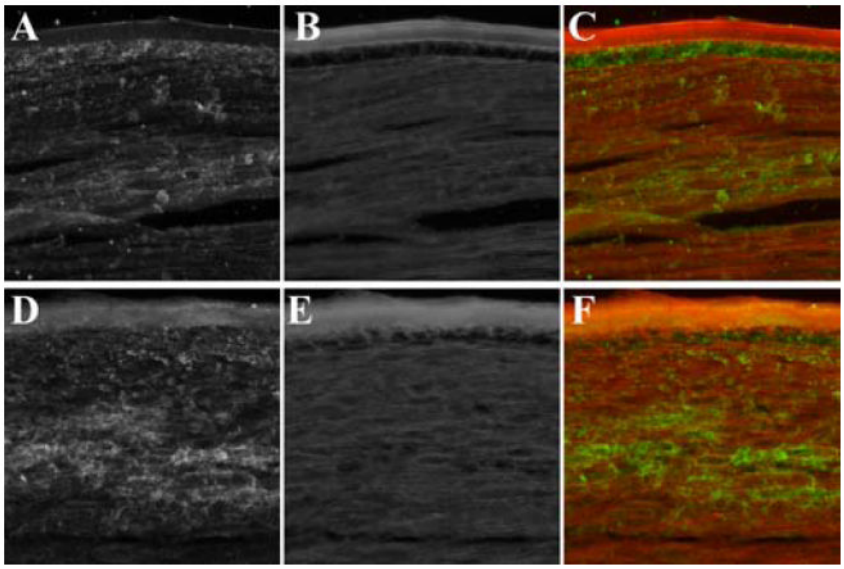

Figure 6.
Glutamate staining in lenses from 4-week-old wild-type (A,B,C) and SPARC-null (D,E,F) littermate animals. The micrographs were of sections through the capsule and lens fibers just anterior to the bow region. Panels (A) and (D) were stained with anti-glutamate. Panels (B) and (E) were counterstained with wheat germ agglutinin conjugated with AlexaFluor-550 to label cell membranes. Panels (C) and (F) were a composite with glutamate in green and wheat germ agglutinin in red. Glutamate staining in the SPARC-null lens decreased in the epithelium and increased in the capsule relative to the wild-type lens. Altered glutamate distribution was consistent with the change in gene expression of glutamate receptors and transporters in the SPARC-null lens and also a general change in the circulation of small molecules.

Table 1

Primer sequences (Invitrogen)

Gene	Forward primer	nM	Reverse primer	nM
C4b	TGCCTTCCGTCTCTTTGAGT	300	TGAAGGCATCTCCTCAATCC	300
Kcne1	TGCAGCCACTGCTTATTTTG	300	ACATGAGGGTGGGAAGAGTG	900
Kng1	GCGAGTACAAGGGCAGACTC	300	TCAGGGTGATGAAGACGATG	900
Serping1	AGCAACACAGGTTCCCAGTC	300	CTGCCAGTTCCTAAGGCTTG	900
Gapdh	AACTTTGGCATTGTGGAAGG	900	ACACATTGGGGGTAGGAACA	900
Socs3	CCTTTGACAAGCGGACTCTC	900	GCCAGCATAAAAACCCTTCA	300

Table 2

TaqMan Gene Expression Assays (Applied Biosystems)

Gene	TaqMan Probe
Adam23	Mm00625643_s1
Gad1	Mm00725661_s1
Gria1	Mm01342712_m1
Pcdh9	Mm03038601_m1
Slc1a1	Mm00436590_m1
Slc2a3	Mm03053806_s1
Slc8a1	Mm00619212_s1

Table 3

Selected genes with altered expression in SPARC-null lenses

Gene expression results. The symbol (*) in the gene symbol column marks genes which have been previously reported in the lens. The symbol (†) in the qRT-PCR column indicates a qRT-PCR p-value <0.05. Fold-change describes the mRNA level in the SPARC-null lens relative to the wild-type lens. A positive number is higher expression and a negative number is lower expression in the SPARC-null lens. The column labeled qRT-PCR indicates fold-change as measured by quantitative RT-PCR.

Fold-change	qRT-PCR	GenBank Accession #	Gene name	Gene Symbol	General function
Ion Channels and Receptors					
-3.05		**BB005970**	Potassium channel, voltage-gated, Isk-related subfamily, member 1	Kcne1	K^+ channel, voltage gated
-3.05	**-1.74**	**BB005970**	Potassium channel, voltage-gated, Isk-related subfamily, member 1	Kcne1	K^+ channel, voltage gated
-2.54		**NM_027398**	Potassium channel-interacting protein 1	Kcnip1	K^+ channel regulator
-2.38	**2.16†**	**U75214**	Solute carrier family 1 (neuronal/epithelial high affinity glutamate transporter), member 1	Slc1a1*	Glutamate transporter
5.05	**2.53†**	**NM_008165**	Glutamate receptor, ionotropic, AMPA1	Gria1	Glutamate receptor, ionotropic
4.06		**BB277244**	Glutamate receptor, ionotropic, kainate 1	Grik1	Glutamate receptor, ionotropic
3.71		**BB313689**	Solute carrier family 8 (sodium/calcium exchanger), member 1	Slc8a1*	Ca^{++} extruded for Na^+ exchange
3.09		**BB130746**	Potassium channel, voltage gated, Shaw-related subfamily, member 1	Kcnc1	K^+ channel, voltage gated
3.08		**U73483**	Calcium channel, voltage-dependent, alpha-2/delta subunit 1	Cacna2d1	Ca^{++} channel, voltage gated
3.01	**2.79†**	**BB414515**	Solute carrier family 2 (facilitated glucose transporter), member 3	Slc2a3*	Glucose transporter
2.97		**BB075134**	Potassium large conductance calcium-activated channel, subfamily M, alpha member 1	Kcnma1	K^+ channel, voltage or Ca^{++} gated
2.72		**AV344554**	Glycine receptor, alpha 1 subunit	Glra1	Glycine receptor, Cl^- channel
2.60		**NM_023868**	Ryanodine receptor 2, cardiac	Ryr2*	Ca^{++} induced Ca^{++} channel
2.49		**BB313857**	Gamma-aminobutyric acid (GABA-A) receptor, subunit beta 2	Gabrb2	GABA receptor, Cl^- channel
2.44		**BB330347**	Glutamate receptor, ionotropic, AMPA4 (alpha 4)	Gria4	Glutamate receptor, ionotropic
2.40		**M92378**	Solute carrier family 6 (neurotransmitter transporter, GABA), member 1	Slc6a1	GABA transporter
2.35		**BB442995**	Potassium channel, voltage gated, delayed-rectifier, subfamily S, member 2	Kcns2	K^+ channel, voltage gated
2.33		**NM_013540**	Glutamate receptor, ionotropic, AMPA2 (alpha 2)	Gria2	Glutamate receptor, ionotropic
2.32		**NM_021398**	Solute carrier family 43, member 3	Slc43a3	Neutral amino acid transporter
2.23		**AV221826**	Sodium channel, voltage-gated, type VIII, alpha	Scn8a	Na^+ channel, voltage gated
2.21		**BC026874**	Solute carrier family 41, member 2	Slc41a2	Cation transporter
2.14	**1.21†**	**AF326547**	Glutamic acid decarboxylase 1	Gad1*	Converts Glutamic acid to GABA
2.10		**NM_008419**	Potassium channel, voltage-gated, shaker-related subfamily, member 5	Kcna5	K^+ channel, voltage gated

Fold-change	qRT-PCR	GenBank Accession #	Gene name	Gene Symbol	General function
2.09		**AI849508**	Sodium leak channel, non-selective	Nalcn	Cation channel, Na^+ leak
Matrix and Adhesion					
-2.36		**NM_021355**	Fibromodulin	Fmod*	Extracellular matrix
-2.18		**NM_011581**	Thrombospondin 2	Thbs2*	Adhesion and migration
-2.06		**U08020**	Procollagen, type I, alpha 1	Col1a1*	Extracellular matrix
-2.03		**NM_010708**	Lectin, galactose binding, soluble 9	Lgals9	Adhesion
3.76	**1.11**	**BQ177394**	Protocadherin 9	Pcdh9	Adhesion
3.51		**AF183946**	Cadherin 10	Cdh10	Adhesion
2.97		**BB386167**	Cadherin 6	Cdh6	Adhesion
2.68	**1.79**†	**AV350138**	A disintegrin and metallopeptidase domain 23	Adam23	Adhesion
2.03		**NM_053144**	Protocadherin beta 19	Pcdhb19	Adhesion
2.02		**BB132137**	Neurexin 3	Nrxn3	Adhesion
Cytoskeleton					
-2.38		**NM_008476**	Keratin 6A	Krt6a	Intermediate filament
2.76		**M20480**	Neurofilament protein, light polypeptide	Nefl*	Intermediate filament
2.76		**AW491150**	MAP/microtubule affinity-regulating kinase 1	Mark1	Microtubule regulator
2.60		**BB750040**	Glial fibrillary acidic protein	Gfap*	Intermediate filament
2.59		**BC018383**	Internexin neuronal intermediate filament protein, alpha	Ina	Intermediate filament
2.46		**AI503514**	CAP-GLY domain containing linker protein 1	Clip1	Microtubule regulator
2.45		**BE947032**	Kelch-like 1	Klhl1	Actin regulator
2.44		**BM200220**	Tau tubulin kinase 2	Ttbk2	Microtubule regulator
2.38		**BB276544**	Midline 1	Mid1	Microtubule regulator
2.03		**BB280360**	Microtubule-associated protein 4	Mtap4	Microtubule regulator
Immune Response					
18.73	**1.84**	**NM_023125**	Kininogen	Kng1*	Inflammatory response
8.32	**14.76**†	**NM_009780**	Complement component 4B	C4b*	Innate immune response
6.83	**4.54**†	**BB241535**	Suppressor of cytokine signaling 3	Socs3	Inhibits cytokine signaling
2.59	**4.24**†	**NM_009776**	Serine (or cysteine) peptidase inhibitor, clade G, member 1	Serping1	Inhibits inflammatory proteases
2.57		**BE992565**	Reticulon 4 receptor-like 2	Rtn4rl2	Inflammatory response
2.14		**Z25469**	Protein S (alpha)	Pros1	Inhibits blood clotting, inhibits inflammation
Cell Signaling					

Fold-change	qRT-PCR	GenBank Accession #	Gene name	Gene Symbol	General function
-2.52		BI465579	Tyrosine 3-monooxygenase/ tryptophan 5-monooxygenase activation protein, beta polypeptide	Ywhab	Regulates many signaling proteins; affects migration
2.78		BB130891	Regulator of G-protein signaling 7 binding protein	Rgs7bp	Regulates GAPs to inhibit Ras G proteins
2.45		AI850720	RAS protein-specific guanine nucleotide-releasing factor 1	Rasgrf1	GEF, activates Ras
2.44		AV347903	Guanine nucleotide binding protein (G protein), gamma 4 subunit	Gng4	Heterotrimeric G protein component
2.07		BM239430	A-kinase anchor protein 13	Akap13	GEF, activates Rho and Rac
Other Notable Genes					
2.37		BB550124	Transglutaminase 2, C polypeptide	Tgm2*	Aggregation, cataract
2.29		AV129500	DnaJ/Hsp40 homolog, subfamily C, member 1	Dnajc1	Chaperone